International Journal of Science and Research (IJSR)
ISSN (Online): 2319-7064
Index Copernicus Value (2013): 6.14 | Impact Factor (2013): 4.438

The Impact of Particles Size Variation of Waste Materials of Heavy Concrete for Gamma Ray Absorption

Ali Basheer Azeez[1], Kahtan S. Mohammed[2], Mohd Mustafa Al Bakri Abdullah[3], Kamarudin Hussin[4], Azmi B. Rahmat[5]

[1, 2,3 ,4,5] Center of Excellence Geopolymer &Green Technology (CEGeoGTech),School of Materials Engineering University Malaysia Perlis (UniMAP), 01000,P.O.Box,D/A Pejabat Pos Besar, Kanger, Perlis, Malaysia, India

Abstract: ***In this study, the dependence of gamma-ray absorption coefficient on the particulate matter sizes of steel slag, iron fillings and steel balls incorporated concrete were examined. The contents of these fillers in concrete mix was kept constant to 35 wt. %. Only the filler particle size was varied during the tests. The particle size ranged from 0.2mm to 1mm for steel slags and the iron fillings and from 2.5mm to 10mm for the steel balls. The concrete samples were assessed for their anti-radiation attenuation coefficient properties. The attenuation measurements were performed using gamma spectrometer of NaI (Tl) detector with Genie 200 software. The utilized radiation source was ^{137}Cs radioactive element with photon energy of o.662 MeV. The results showed that gamma-ray attenuation coefficient was inversely proportional to the filler particulate matter size. Likewise the mean free paths for the tested samples were obtained. Maximum linear attenuation coefficient of 1.102±0.263cm^{-1} was attained for the iron filling. The iron balls and the steel slags showed much inferior values. The concrete incorporates iron fillings afforded the best shielding effect. The density, microstructure, homogeneity and particulate distribution of the concrete samples were examined and evaluated using different metallographic, microscopic and measurement facilities.***

Keywords: Attenuation coefficient, gamma ray, wastes materials, particles size, NaI (Tl).

1. Introduction

Radiation shielding commonly used to protect medical patients and workers from exposure to direct and secondary radiation during diagnostic imaging in hospitals, clinics and dental offices. The effectiveness of radiation shielding varies significantly with the attenuation coefficients of the constituent materials, the thickness of the material and the energy spectrum of the radiation [1].To insure total safety, all radioactive materials in the laboratory or place of work should be surrounded by sufficiently thick shielding material such that the radiation in neighboring work areas is kept at minimum permissible levels. This quantity of shielding is determined by the material chosen. The choice of shielding materials and the design of the shield depends on the type of radiation and its intensity. While certain materials suite better than others for a given type of radiation, cost usually limits the choice of shielding to a few readily available materials. The most used are lead, iron and steel, Lead is often used because of its high atomic number and density, but it has significant disadvantages toxic, not environment-friendly and there are several attempts to replace the shield by environment-friendly materials. [2].

There are three general rules for protection: exposure time, distance, and shielding. In most cases, shielding is the main rule to be performed [3] although materials such as lead [4] and iron are effective anti-ray shields, mechanical and economical considerations limit their usage to some special areas. On the other hand concrete is one of the most important materials used for radiation shielding in facilities containing radioactive sources and radiation generating equipment [5].

The problem of shielding against ionizing radiation has always attracted a great deal of attention. Radiation shielding of a nuclear reactor is a costly and very complex process [6] .A nuclear reactor usually requires two shields; a shield to protect the walls of the reactor from radiation damage and at the same time reflect neutrons back into the core and a biological shield to protect people and the environment.

2. Experimental

Table 1 shows the three size ranges of the waste particulates used, to fabricate the three concrete sample sets. The filling wt. % of these waste materials in the concrete sample sets were kept constant to 35 wt. %.

Table 1: The particle size of the concrete fillers

Material	Iron filling	Iron balls	Steel slag
particle Size	0.2mm	2 mm	0.2mm
	0.5mm	5 mm	0.5mm
	1 mm	10 mm	1 mm

Linear attenuation coefficients measurements were performed for each sample using gamma ray spectrometer of 3”×3” NaI (Tl) detector with a Multi Channel Analyzer (MCA)[7,8]. The spectrometer communicates with the PC by Genie200 software. The waste particulates were refined and sieved to give different sizes ranging from 0.2mm to 1mm for the iron fillings and the steel slags and 2.5mm to 10 mm for the steel balls. The concrete−waste materials mixture was mixed for 20minutes which considered enough to achieve good homogeneity [9]. The emitting energy of the utilized ^{137}Cs source was of 0.662MeV. The (μ) for the tested samples were experimentally determined using narrow collimated mono-energetic beam of gamma– rays. The schematic description of the experimental setup is shown in figure. 1.

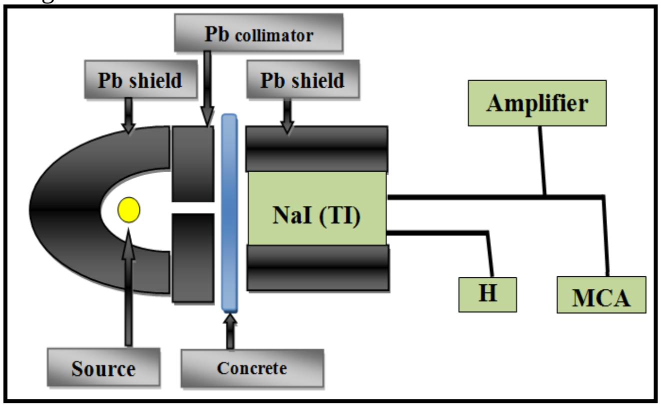

Figure 1: Schematic representation of the setup of the measurements

3. Calculations

The background was subtracted from the initial intensity (*Io)* and the Intensity *(I)* of the transmitted beam .The density (ρ*)* is the mass and volume dependant. The μ was determined by measuring the transmission of gamma-rays through samples a target of known thickness. Gamma ray spectrum for ^{137}Cs is show in figure. 2. The single sharp peak related to the ^{137}Cs source of 0.662 MeV ray is show in figure 2.

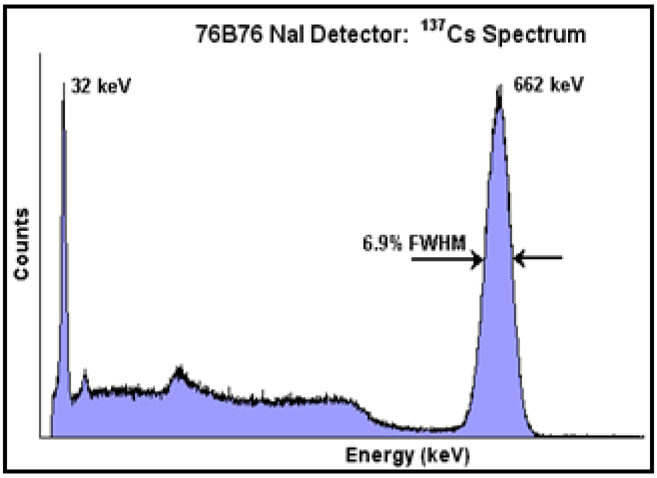

Figure 2: Gamma ray spectrum obtained from ^{137}Cs source.

The area under the curve of the photo peak spectrum is used to evaluate the intensity *I* of the transmitted beam. Evaluation of the I_o which is the area under the photo peak is obtained without inserting any sample between the detector and the source, from *I* and the incident photon *Io* for a thickness *x* of the absorber, the μ is given by the following formula:[10].

$$\mu = \frac{1}{x} ln\frac{Io}{I} \qquad \text{Eq. 1}$$

Eq.1 is valid only if two conditions are satisfied. First; the photons of the incident beam are mono-energetic. Second, the beam must be narrow. For broad beam source geometry or thick shield, usually another term is introduced to Eq.1 called the buildup factor B [11].Additionally, the density *(*ρ*)* of the of the concrete-iron fillings samples having the highest density and the best attenuation results was calculated by following the rule of mixture. Ordinary black Portland cement was used to prepare the tested samples. The shielding properties of these types of concretes have been investigated. These samples of concrete mixes were produced according to ASTM no C637[12].Reference concrete mixes design ratio 1:2:4 consisted of cement 5kg/m^3, sand 10kg/m^3, gravel 20kg/m^3, and water 2kg/m^3 were utilized. The water to cement (w/c) ratio was 0.39. Figure 3(a-b) shows the cross sectional low magnification optical macrograph of concrete mould of 35 wt. % iron filling waste exhibits the distribution of the iron particles within the concrete matrix and optical graphs of attenuation test samples with different waste materials respectively.

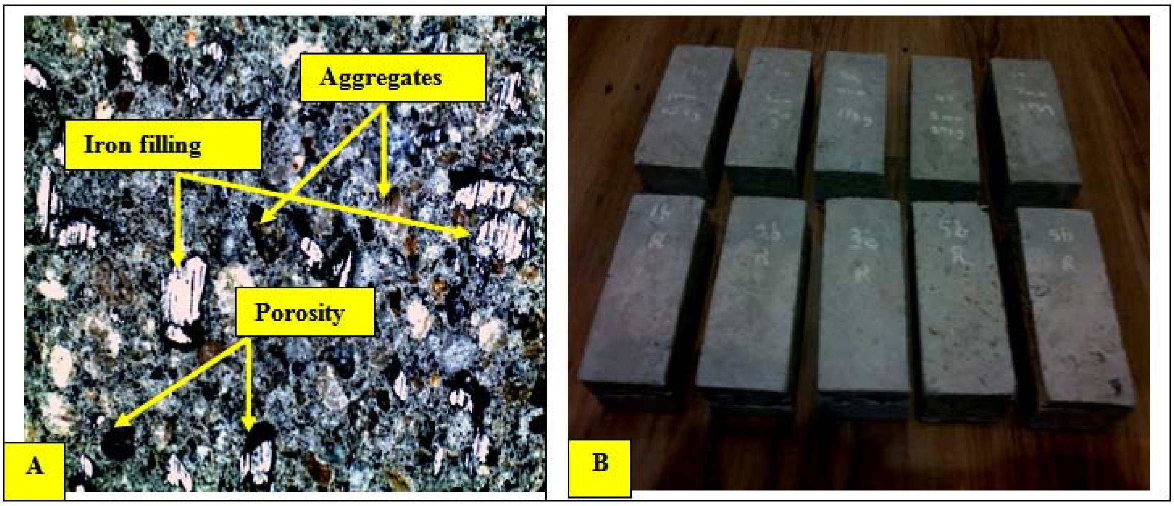

Figure 3: (A) cross sectional low magnification optical macrograph of concrete mould of 35 wt. % iron particulates waste exhibits the distribution of the iron filling within the concrete matrix (B) optical graphs of attenuation test samples with different waste materials.

The gamma-ray spectrum was acquired for a real time of 60 s for each measurement which was reasonably enough to obtain a good high distribution pulse. Attenuation coefficients were determined by graphical method, in which the slope of the fitted line to the plot of radiation transmission rate given by ln (Io/I) versus sample thickness x gives the total linear attenuation coefficient as shown in figure 4.

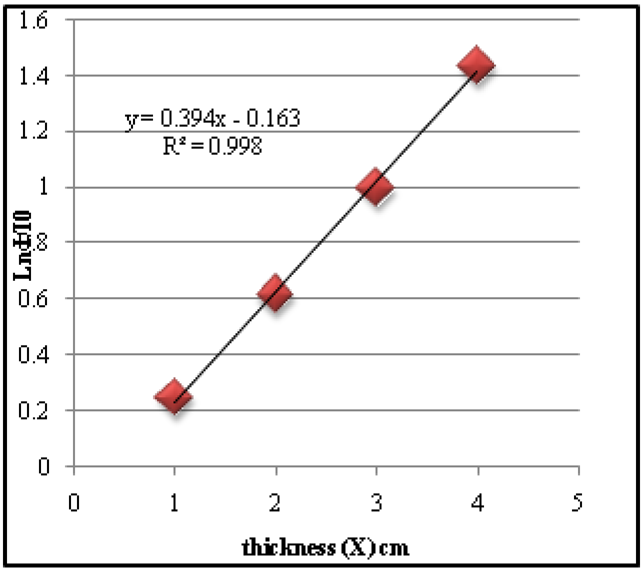

Figure 4: linear attenuation coefficients from the measured I and I_o values as a function of the sample thickness for the ^{137}Cs source.

The values of the standard deviations at eight positions for each fabricated sample were calculated using the following formula:

$$\sigma(\bar{\mu}) = \frac{\sqrt{\Sigma(\mu l-\bar{\mu})^2}}{N-1} \qquad \text{Eq. 3}$$

Where; σ ($\bar{\mu}$) is the standard deviation at any position, $\bar{\mu}$ is the average values of (μ) and N is the number of the measured positions for each sample, 8 positions were measured for each sample to calculate the standard deviation. The half value level (HVL) for the fabricated samples of combined waste material of different granule sizes was calculated according the following formula;

$$\text{HVL} = 0.693/\mu \qquad \text{Eq. 4}$$

whereas HVL is the average amount of material needed to absorb 50% of all radiation**,** it is related to mean free path, however the mean free path (*mpf*) of a pencil beam of mono-energetic photons is the average distance that the photon travels between successive collisions with the atoms of the absorbed material. It depends on the material and the energy of the photons, *mpf* was calculated using the following formula:

$$mpf = \mu^{-1} = ((\mu/\rho)\rho)^{-1} \qquad \text{Eq.5}$$

Where; μ/ρ is the mass attenuation coefficient and ρ is the density of the material.

4. Results and Discussion

The measured average values of (μ), their standard deviation, the half value level and the mean free path for the three sets of concrete samples are given in Table 2.It is clear from Table2 that the values of the standard deviations are small and varied from 0.02 to 0.2. This gives good indication that the fabricated samples have good homogeneity and even distributions of the dense components within the concrete cohesive mixture. The value for the (μ) of the fabricated samples were increased as the filler particulate size decreases. Samples of iron fillings incorporate concrete gave higher attenuation values of about 11% as compared to the other tested samples under similar testing conditions i.e. utilization of ^{137}Cs radioactive source of 0.662 MeV. The HVLs were inversely proportional to the (μ) values.

International Journal of Science and Research (IJSR)
ISSN (Online): 2319-7064
Index Copernicus Value (2013): 6.14 | Impact Factor (2013): 4.438

Table 2: The average linear attenuation coefficient (cm^{-1}) with the standard deviation, HVL in cm and the mfp in cm for the tested samples

Material	Particulates size parameters	1 mm	0.5 mm	0.2mm
Iron filling (sample 1)	$\bar{\mu}$ (cm^{-1}) And $\sigma(\bar{\mu})$	0.724±0.053	0.876±0.0652	1.102±0.263
	HVL (cm)	0.957	0.791	0.628
	Mfp (cm)	1.381	1.141	0.907
Steel slag (sample 2)	$\bar{\mu}$ (cm^{-1}) And $\sigma(\bar{\mu})$	0.495±0.063	0.601±0.079	0.883±0.032
	HVL (cm)	1.401	1.153	0.784
	Mfp (cm)	2.020	1.663	1.132
Steel ball (sample 3)	Particulates sizes parameters	**10 mm**	**5 mm**	**2.5 mm**
	$\bar{\mu}$ (cm^{-1}) And $\sigma(\bar{\mu})$	0.529±0.037	0.631±0.0451	0.871±0.021
	HVL (cm)	1.310	1.098	0.795
	Mfp (cm)	1.890	1.584	1.148

The *mfp* decreased as the (μ) increased. Small *mfp* values means higher numbers of interactions by the incident radiation beam with the atoms of the shielding material i.e. small distance between two successive collisions which eventually gives large attenuation levels, this clear from figure 5. The (μ) of concrete-waste samples incorporate different filler particle sizes were measured. The results were displayed in Fig.6 for the source ^{137}Cs; it can be seen from this figure that the (μ) increased with the decreasing of particle size for waste material contents within concrete samples.

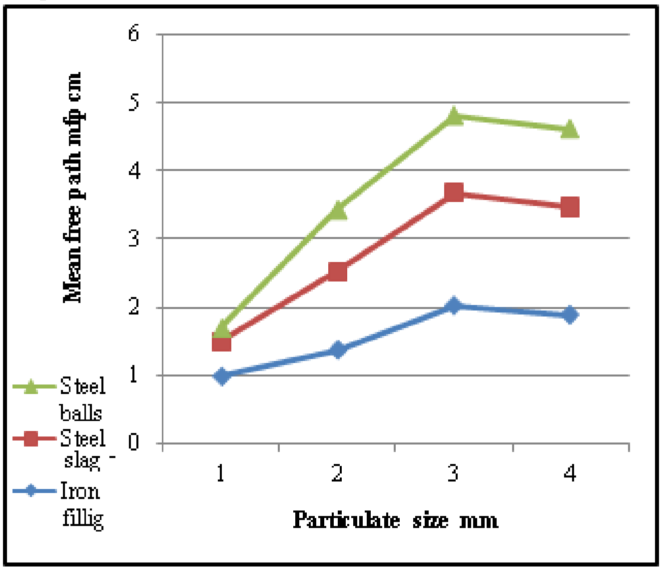

Figure 5: The Mean free path as a function of the additives particle size

The correlation between the (μ) and the particle size of the waste materials in the concrete is used to confirm the linearity. It is obvious that samples of small particle size and high dense waste material component are effective in preventing the transmission of radiation. Figure 7 elucidate a big particle size absorber, which have a large blank between particles and the small particle size which have small blanks between particles. When the incident radiation beam enters each absorber the particles of small size present larger targets for the radiation to strike and hence the chance for interaction via the Photo electric and Compton effects is relatively high. The attenuation should therefore be relatively large. In the case of the big particle size absorber the blanks between particles are large and hence the chances of interactions are reduced. In other words, the radiation has a greater probability of being transmitted through the absorber and the attenuation is consequently lower than in the small particle size case.

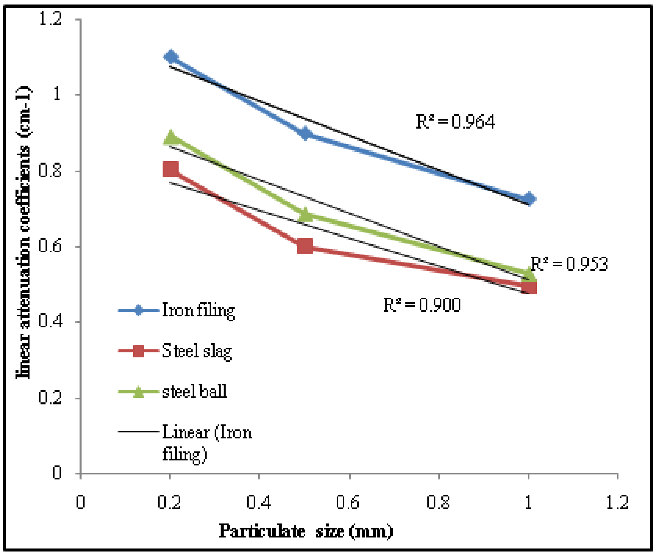

Figure 6: The linear attenuation coefficients as a function of the additives particle size.

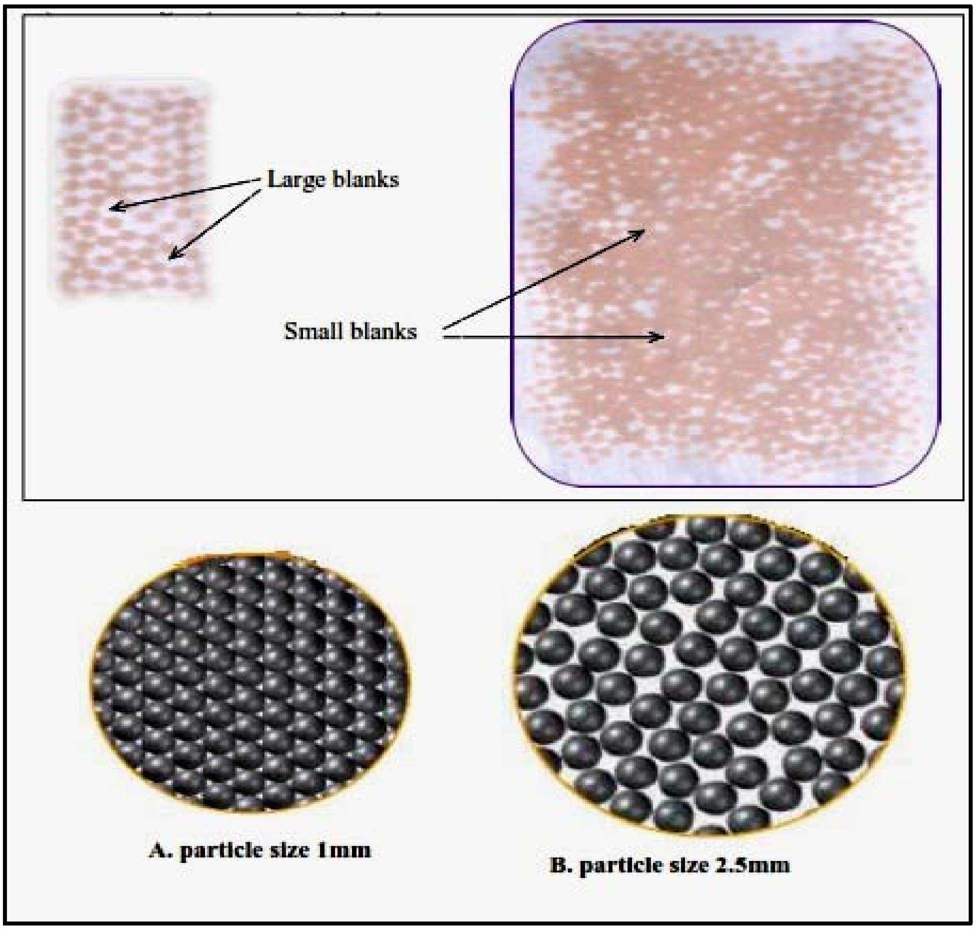

Figure 7: Particles for the same weight but different size

5. Conclusion

The results showed that gamma-ray attenuation coefficient is inversely proportional to the additives size. This is attributed to the close packing levels of the additives within the sample. The (μ) increased with increasing of density and decreasing granular size for waste materials content in the concrete samples. The packing level of large additives is inferior to that for additives of smaller granule size. The radiation has a greater probability of being transmitted through the absorber and the attenuation is consequently lower than in the small particle size case. Furthermore, the radiation is drastically reduced when the samples have high distribution of waste material particles. All above mentioned parameters lead to increase the attenuation by increasing the capability of shield material and radiation interaction.

References

[1] Hayder S. Hussain Abdel hussainA.Al-BayatiHarith I. Jaffer Baghdad Science Journal Vol.8(2)2011 .Dependence of gamma-ray absorption coefficient on the size of lead particle.
[2] IAEA Treatment Machines For External Beam Radiotherapy. Chapter 5, in IAEA Radiation Oncology Physics: A Handbook For Teachers And Students. International Atomic Energy Agency, Vienna,(2005).
[3] G. Eaves, Principles of Radiation Protection, Iliffe Books Ltd, London,(1964).
[4] I. Akkurt, H. Akyıldırım, B. Mavi, S. Kılınçarslan,C. Basyigit, Ann. Nucl. Energy 37, 910; (2010).
[5] Concrete Singh, K.J., Singh, N., Kaundal, R.S., Singh, K., Gamma-ray shielding and structural properties of PbOeSiO2 glasses. Nuclear Instruments and Methods in Physics Research B 266, 944e948 (ELSEVIER)(2008).
[6] Pavlenko VI, Yastrebinskii RN, Voronov DV Investigation of heavy radiation-shielding concrete after activation by fast neutrons and gamma radiation. Journal of Engineering Physics and Thermophysics, 81: 1062- 0125;(2008).
[7] Production of a datolite-based heavy concrete for shielding nuclear reactors and megavoltage radiotherapy rooms Iran. J. Radiat. Res. 8 (1): 11-15S.M.J. Mortazavi1*,M.A. Mosleh-Shirazi2,M.Baradaran-Ghahfarokhi3,Z. Siavashpour3, A. Farshadi3, M. Ghafoori4, A. Shahvar4(2010).
[8] ASTMC637: Standard specification for radiation shielding concrete, (1998).
[9] S. Kilincarslan, I. Akkurt, C. Basyigit, Mater. Sci.Eng. A 424, 83 (2006).
[10] Stark, David, and Klieger, Paul, Effect of Maximum Size of Coarse Aggregate on D-Cracking in Concrete Pavements, Research and Development Bulletin RD023,Portland Cement Association, (1974).
[11] I. Akkurt, H. Akyıldırım, B. Mavi, S. Kılınçarslan,C. Basyigit, Radiat. Measurem.45, 827 (2010).
[12] ***, ASTM C637: Standard specification for radiation shielding concrete, 1998.